Distribution Agreement

In presenting this thesis as a partial fulfillment of the requirements for a degree from Emory University, I hereby grant to Emory University and its agents the non-exclusive license to archive, make accessible, and display my thesis in whole or in part in all forms of media, now or hereafter now, including display on the World Wide Web. I understand that I may select some access restrictions as part of the online submission of this thesis. I retain all ownership rights to the copyright of the thesis. I also retain the right to use in future works (such as articles or books) all or part of this thesis.

Elias Heanue November 10, 2024

Electrical perturbation of solvent dynamics by using an open-ended coaxial probe

by

Elias Heanue

Kurt Warncke, Ph.D

Adviser

Physics

Kurt Warncke, Ph.D

Adviser

Jed Brody, Ph.D

Committee Member

Wladimir Benalcazar, Ph.D

Committee Member

2024

Electrical perturbation of solvent dynamics by using an open-ended coaxial probe

by

Elias Heanue

Kurt Warncke, Ph.D

Adviser

An abstract of
a thesis submitted to the Faculty of Emory College of Arts and Sciences
of Emory University in partial fulfillment
of the requirements of the degree of
Bachelor of Science with Honors

Physics

2024

Abstract

Electrical perturbation of solvent dynamics using open-ended coaxial probe
by Elias Heanue

Enzyme function is intimately related to motions in the surrounding solvent environment. Ethanolamine ammonia-lyase from *Salmonella typhimurium* exemplifies an enzyme in which a select class of solvent-coupled protein configurational fluctuations is obligatory for physiological activity. The ability to drive specific classes of solvent-coupled protein fluctuations by using an electric field oscillating at microwave frequencies provides a mechanism for actuating and characterizing the solvent-protein dynamical coupling. As a first step, we design a microwave circuit and test system to probe the dynamics in aqueous solution, by using an open-ended coaxial probe to deliver microwave radiation to interstitial solvent domains in frozen solution samples (200 - 240 K) in the frequency range of 1.0 - 1.6 gigahertz, with a maximum power of 2 Watts. Continuous-wave electron paramagnetic resonance (EPR) spectroscopy is used for reporting on the solvent dynamics through the rotational mobility of the nitroxide spin probe, TEMPOL. We design a circuit featuring a circulator component, which allows for delivery of microwave power to the sample via the coaxial probe, while reporting on the power absorption by the sample. A microwave power- and frequency-dependent increase in amplitude and associated narrowing of the EPR spectra is observed, which indicates increased mobility in the solvent. The devised twin capabilities of microwave actuation and sensitive detection of solvent motion signify the ability to characterize the role of select, gigahertz-frequency fluctuations in enzyme catalysis.

Electrical perturbation of solvent dynamics using open-ended coaxial probe

by

Elias Heanue

Kurt Warncke, Ph.D

Adviser

A thesis submitted to the Faculty of Emory College of Arts and Sciences
of Emory University in partial fulfillment
of the requirements of the degree of
Bachelor of Science with Honors

Physics

2024

Acknowledgements

I would like to acknowledge my adviser Dr. Kurt Warncke for being an insightful and patient mentor to me. I would like to thank the graduate students in the lab - Katie Whitcomb, Shaady Fouad, Hana Alsheikh, and Dr. Wei Li - for their guidance and support. In addition, I would like to give thanks to Lowell Ramsay for his continuous support with technical details. Finally, thank you to my committee members Dr. Jed Brody and Dr. Wladimir Benalcazar for their time.

Table of Contents

List of figures

Introduction

I. Microwave effects on enzyme activity

Microwave irradiation has been used conventionally for heating over nearly the past century, owing to its speed. While conventional heat sources rely on a conductive out-to-in trajectory, microwave sources are able to heat the sample by directly actuating motion of charges and dipoles in the body of the material[1]. Along with its efficiency advantage, this microwave heating has been accompanied by unexpected results. In the 1980s, it was revealed that under microwave irradiation, there are significant rate enhancements in certain organic synthesis reactions[2]. Along with rate enhancements, enzyme samples subject to microwave irradiation have also been shown to perform physiological function in environments that would typically render catalysis effectively inactive, including chemically harsh chloroform solvents and temperatures significantly below physiological values[3,4]. Determining the source of these unpredicted behaviors has been difficult, since it is hard to distinguish between thermal effects and a "microwave-specific" property. However, in certain cases the impact of microwave radiation has been separated from purely thermal effects through systematic determination that changes in the sample's physical properties are not explained through thermal effects alone[5]. The notion of a "rotational temperature" has been proposed, where the continuous microwave radiation incident on dipolar solvent molecules leads to a fast, and therefore rotationally "hot," local pockets within the solution, fundamentally changing how solvent molecules interact with enzymes within the sample[6-8]. While this approach does give an explanation for unconventional thermal activity, it ignores interactions between the protein and solvent, disregarding the potential connection of the protein to the surrounding molecules. Protein motions are intimately

coupled to their environment[9,10], so there is a need to understand the relation between this strong coupling and the "microwave-specific effect." At this point, the exact mechanism of microwave-specific rate enhancement is not fully understood. We find that application of microwave power to our solvent results in a detectable increase in mobility within the solution, consistent with detected increases in temperature from other studies. This effect is correlated positively with the applied power and displays a trend of increase with the frequency of radiation.

II. Ethanolamine ammonia-lyase as an example system

Ethanolamine ammonia-lyase, a coenzyme B-12 dependent bacterial enzyme responsible for the catalysis of the conversion of ethanolamine to acetaldehyde and ammonia, conducts its enzymatic activity through a choreography of chemical events within its active site[11]. In previous EPR studies, the molecular motions that actuate catalysis in this active site have been related to specific, or "select," fluctuations of the solvent immediately surrounding the protein. Below a certain temperature (dependent on the cryosolvent used), there is an ordering transition in the protein-associated domain of solvent, or hydration layer, that quenches the collective cluster class of solvent fluctuations on the time scale of the enzyme reaction. The absence of these motions disables the enzyme from conducting its native reaction, resulting in a splitting of the physiological reaction into two separate kinetic processes, resulting in a bifurcation of the reaction pathway. This behavior indicates a dependence of the native enzyme catalysis on 'select' motions in the solvent[12]. Because of this dependence, inducing these select fluctuations in the solvent may drive the enzyme process, thus leading to an increased reaction rate.

III. Open-ended coaxial probe technique

While conventional microwave ovens are able to heat a large amount of sample simultaneously and quickly, they do not report on what is happening within the sample as it is being heated. In contrast, open-ended coaxial probes can be used to both deliver microwave irradiation to a small region of the sample and detect changes in its dielectric properties[5, 13,14]. The proportion of reflected microwave energy is sensitive to the dielectric (permittivity) properties of the sample, and these properties are dependent on the temperature of the sample in the region of the probe. Open circuit coaxial probes have been used in medical and industrial settings as a local, sensitive detection device; their ability to detect slight shifts in dielectric permittivity has been exploited to measure where regions of organic tissue change and where pocket defects occur in manufactured goods without penetration of the target subject[13, 14]. Along with their sensitivity , these probes also have the benefit of being relatively small-scale devices. This size provides a versatility for these probes to be used in otherwise inconvenient settings, where the sample is restricted to a small or relatively inaccessible space. The small size also allows for introduction of the probe to small, millimeter-scale sample tubes and the ability to function concurrently with compatible experimental apparati without posing a major inconvenience spatially.

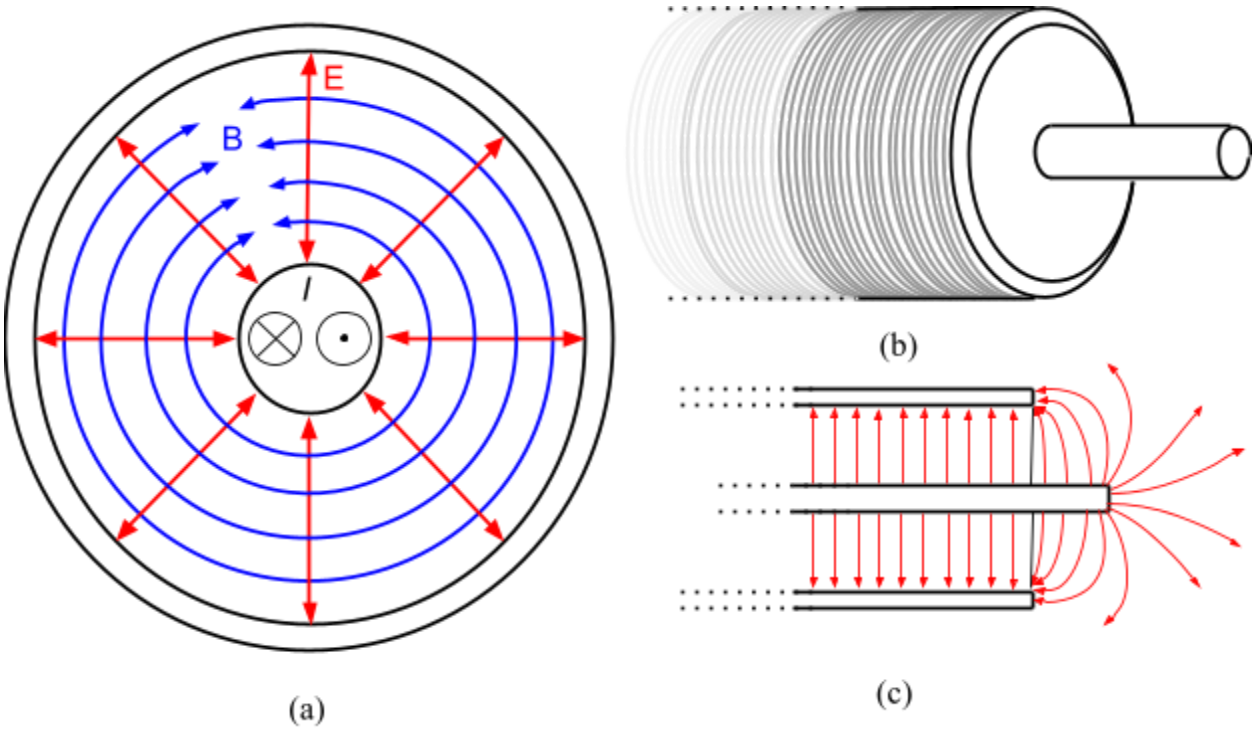

Figure. 1 Visual representations of the open-ended coaxial probe and accompanying electric (*E*) and magnetic (*B*) fields. The cable is made up of a center conductor surrounded by a layer of insulating material and sheathed by a grounded outer conductor. The signal is transmitted via the center conductor. (a) Cross-section representation of the *E*-field and *B*-field at moments where the alternating current is traveling into and out of the page, causing directional changes of the *B*-field. (b) Three-dimensional representation of the probe tip, with concentric rings showing the surface of the outer conductor. (c) Side-view schematic of the *E*-field lines (red), showing shielded coax interior region and the exit and reentry of *E*-field lines in the region of the probe tip.

IV. Electron paramagnetic resonance (EPR) spectroscopy

EPR spectroscopy allows for an observation of the mobility of the solvent. Solvent dynamics are reported by the nitroxide spin probe TEMPOL, which carries a single electron spin, (S=1/2), associated with the nitroxide function. Changes in the solvent dynamics are manifested in line shape changes of the first-derivative absorbance spectrum. In protein systems, changes in the line-shape can be extrapolated to the characteristic motion in different solvent regions[15-17]. Resonance peaks result from energy level splitting from interactions between the unpaired electron and the external magnetic field, as well as the hyperfine interaction of the electron with its associated nuclei. With TEMPOL, the unpaired electron resides partially on ^{14}N (I=1), giving rise to three peaks in the spectrum (m_I=0, ±1). Due to limitations of appropriate sample size, cavity size and field strength, the EPR spectrometer operates at X-band (8-12 GHz) microwave frequencies. The particular microwave frequency used in the experiments was 9.5 GHz. In the X-band frequency range, the ^{14}N hyperfine interaction has a dominant effect, allowing for distinguishable differences in line shape accompanying altered mobility of TEMPOL. At sufficiently low temperatures (TEMPOL rotational correlation time, $\tau_C \geq 10^{-7}$ s) the rigid limit of measurement occurs, and the EPR spectrum displays the "powder-pattern" line shape. As temperature increases, the dipolar hyperfine interaction becomes rotationally averaged, causing a narrowing of each of the three m_I lines and thus a sharpening of the EPR spectrum. System measurement at high temperatures reaches a limited resolution at correlation times $\tau_C < 10^{-10}$ s.

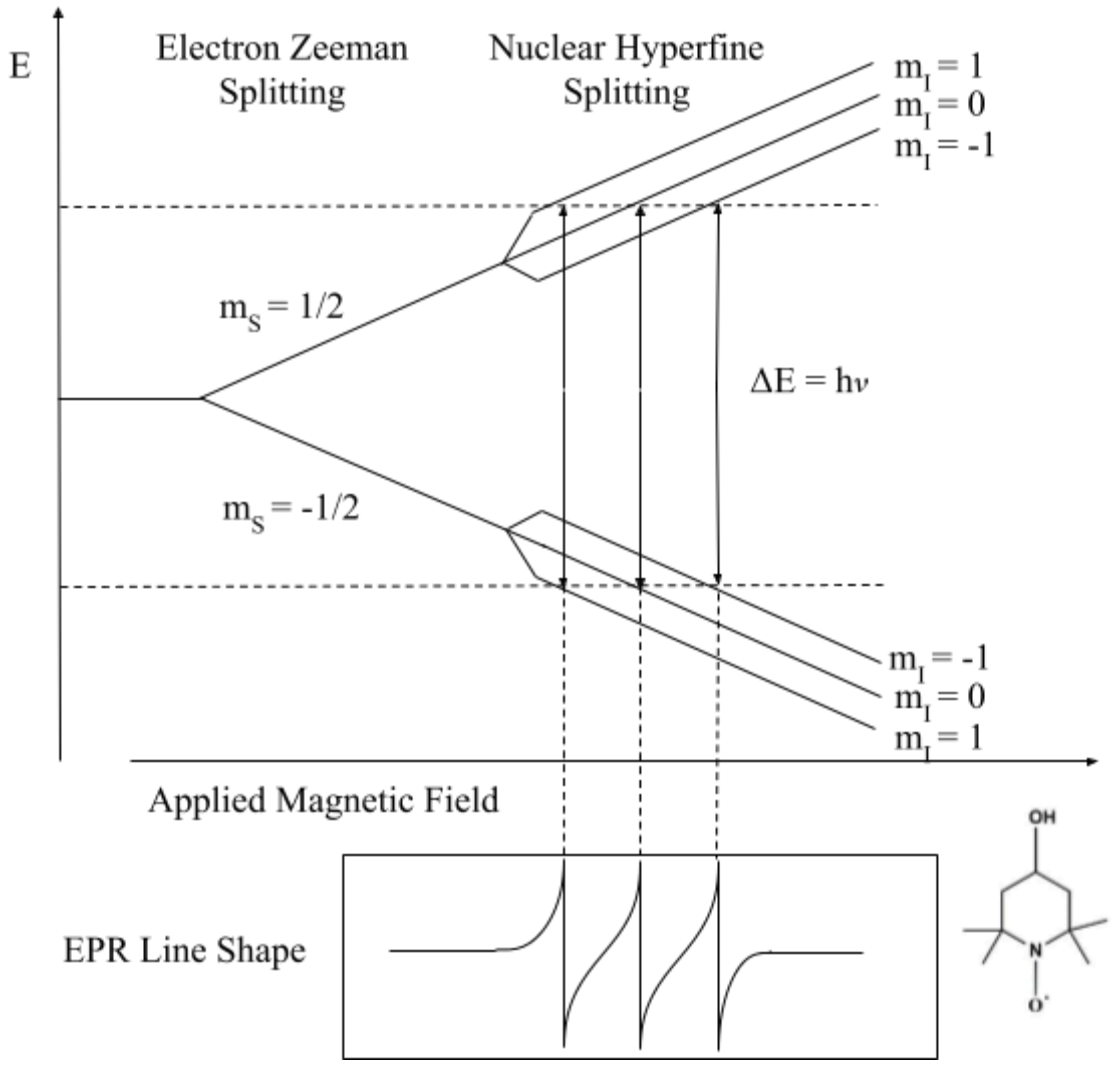

Figure. 2 Energy level splitting diagram for the TEMPOL EPR spin probe (structure, bottom right). In the presence of a magnetic field, there is a splitting between m_S=+½ and m_S=-½ states. Further splitting results from the hyperfine coupling of TEMPOL's ^{14}N with associated nuclear spin values m_I=0,±1. The constant microwave frequency (ν) within the cavity gives three applied magnetic field values where the resonance condition $\Delta E = h\nu = g_e\beta H$ is met, where h is Planck's constant, g_e is the electron g factor, β is the Bohr magneton, and H is the applied field magnitude. As represented through the connecting vertical dashed lines, each H value where this condition is met corresponds to resonant absorbance of microwaves. The derivative shape of the lines is caused by the use of phase-sensitive detection as a technique to enhance the signal.

V. Circuit design

To simultaneously deliver the actuating microwave radiation (1.0 - 1.6 GHz), measure the reflected microwave power, and report on real-time dynamics of the solvent and the effects of microwave perturbation, through the motion of the spin probe (EPR performed at 9.5 GHz microwave frequency), we designed a circuit to operate the open-ended coax probe (RG402) in contact with the sample within the resonator (SHQE; Bruker, Billerica, MA) EPR spectrometer (E500; Bruker). The circuit depicted in Figure 3 features a broadband (0.01-20 GHz) microwave source (83752A; Hewlett-Packard) that sends microwave power to the sample and ultimately to a spectrum analyzer (8590A; Hewlett-Packard) that reports the power spectrum of the reflected signal. The signal experiences a 35 dB amplification (PE15A4025; Pasternack) before passing through an isolator (PE8300; Pasternack). A circulator (PE8400; Pasternack) directs the power to the sample, and any reflections are attenuated by a 10 dB fixed attenuator (XMA, Manchester, NH) before being delivered to the spectrum analyzer. The 17 dB isolator following amplification is placed before the circulator to protect both the amplifier and the microwave source from any reflections in the system. All circuit elements have a 50-ohm characteristic impedance to minimize loss in element contacts. The semi-rigid coaxial probe is in direct contact with the sample, which rests vertically in the center of the cavity resonator for measurement. Bandwidth limitations among components of the collective circuit limit probe signals to a power range of 20-33 dBm and a frequency range of 1-1.6 GHz (L-band microwave bandwidth).

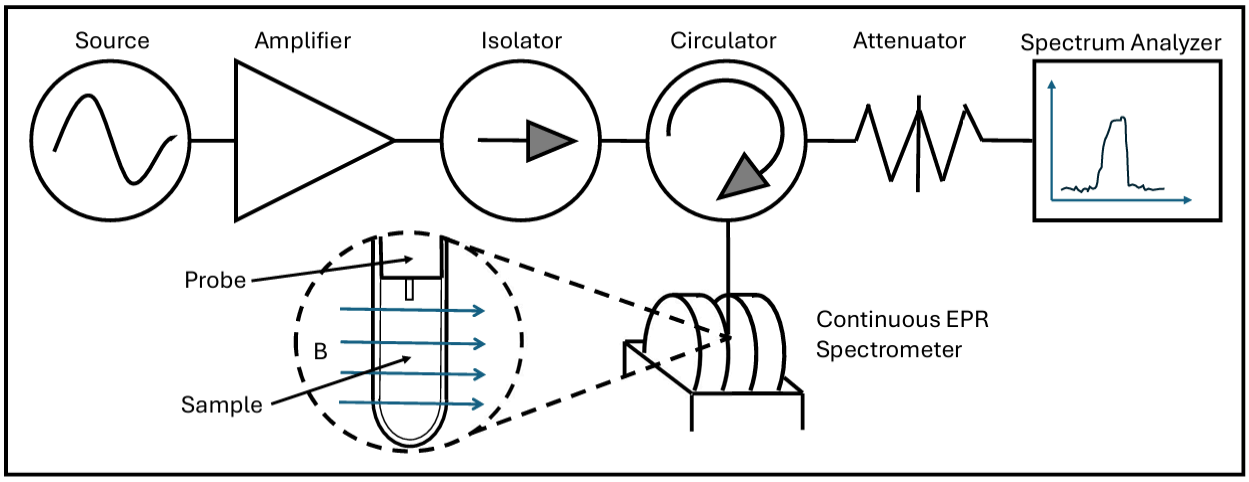

Figure 3. Circuit diagram of experimental apparatus for the electrical perturbation of samples concurrent with continuous-wave EPR measurements. A microwave synthesizer routes a signal through a 35 dB amplifier. The circuit features a circulator component, which allows for the directionally specific path of the input signal to the probe, and routing of the reflected portion of the signal from the probe to the spectrum analyzer. Here, the microwave signal is delivered to the sample, resting in the resonance cavity of the EPR spectrometer, between the pole faces of the electromagnet. The dashed lines outline a zoomed-in frame depicting the probe within the sample tube in contact with the solution. After the signal is carried to the sample, any reflected power is passed through the circulator to a spectrum analyzer where the power reading is displayed.

VI. Motivation

A full mechanistic understanding of microwave effects on enzyme activity remains elusive. Microwave radiation is understood to interact with charges in solution, both through ionic conduction (translation) and dipolar rotation. "Select" solvent fluctuations have been shown to be directly coupled and obligatory for enzyme activity in EAL, which offers a system amenable to sensitive measurements of kinetics through time-resolved, continuous-wave EPR spectroscopy. Here, the goal is to actuate and detect effects on solvent mobility owing to microwave radiation in the 1.0 to 1.6 GHz range. Achieving detectable changes in the dynamics of the TEMPOL spin probe in solution as a result of microwave perturbation would indicate an ability of our probe to influence motion within the system.

Methods

I. Sample preparation for dielectric property change measurements

Chemicals used were commercially sourced. Measurements made using RG174 flexible coax were performed in 4mm quartz EPR samples tubes (Wilmad, NJ) cut to 7 cm lengths. Temperature control was achieved with high-purity nitrogen gas cooled by a dry ice-ethanol bath.

II. EPR Sample preparation

EPR samples were prepared in 5 mm quartz NMR tubes. EPR samples contained 0.4 ml solution containing 10 mM potassium phosphate buffer (pH, 7.5), 2 % v/v DMSO. Sample was frozen in a two-step process. First, 200 µL solution without TEMPOL spin probe was frozen in isopentane at 140 K. Then, 200 µL containing 200 µM TEMPOL was deposited onto the frozen solution. The semi-rigid coaxial probe tip was then inserted, such that the outer dielectric was flush with the solution surface, and the sample and probe were submerged in the cold isopentane until frozen. Samples were then transferred to and held in liquid nitrogen until the EPR measurement.

III. Cooling bath and temperature control experiments

Salt data was collected from samples suspended in an ethylene glycol cooling bath. Measurements made in the bath were done with RG402 semi-rigid coax. Sample volume was set to 30 mL and 0.2% v/v NaCl was added followed by vortexing for 15-30 s. The semi-rigid coaxial probe was partially submerged in the bulk solution, centrally located with approximately

1 cm depth below the solution surface. Temperature was monitored by a type T thermocouple submerged at similar depth. At each temperature, the solution was held until measurement values were constant over long timescales (> 1 minute).

IV. Continuous wave EPR spectroscopy

EPR spectroscopy was performed on a Bruker E500 ElexSys EPR spectrometer using the ER 4123SHQE X-band cavity resonator. Spectroscopy was performed in the X-band frequency range, with microwave frequency near 9.5 GHz; measurements were performed with 0.2 mW applied microwave power. Four spectra were everaged for each temperature-frequency-power combination.

V. Application of probe microwave power

Microwave radiation was produced using a Hewlett Packard 83752A synthesized sweeper, and the real-time power spectra from reflected signals were monitored on the Hewlett Packard 8590A spectrum analyzer. The spectrum analyzer is calibrated for appropriate amplitude and frequency measurements with a test signal of 300 MHz at a power level of -20 dBm. For power dependence measurements, the circuit was set to minimum power output and then raised to higher powers at each temperature.

Results

I. Detection of differences in dielectric properties with the open-ended coaxial probe

RG-174 flexible coaxial cable was used for preliminary tests of probe sensitivity. With direct connection to the spectrum analyzer, this probe detected differences in the medium it was in contact with, as depicted in Figure 4. In contact with air, less power from the 0 dBm radiation was absorbed when compared with contact with water. This result was true across the frequency range of 1.0-2.0 GHz. At high frequency (near 2.0 GHz), there is a significant decrease in reflected power from the probe in both media.

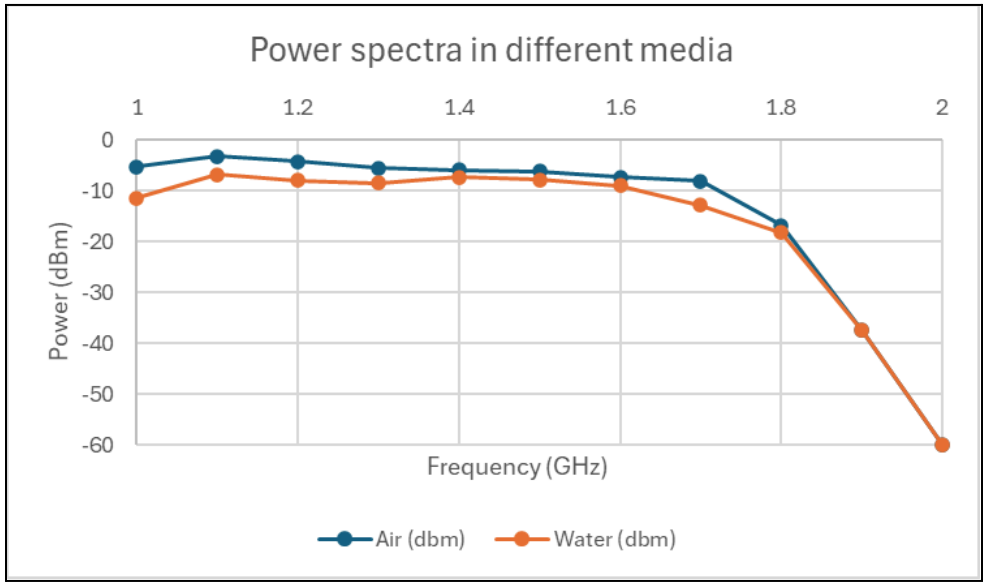

Figure 4. Power spectra from open-ended flexible probe in contact with air (blue) and water (orange). Water showed the ability to absorb more power from the 0 dBm source than air across all frequencies in the 1-2 GHz band. General decrease in signal at higher frequencies is attributed to the bandwidth limitation of the spectrum analyzer (1.5 GHz maximum recommended input). Measurements made at room temperature (~21 °C, 294 K).

Semi-rigid RG-402 coaxial cable was used for all later experiments In bulk samples, measurements of the reflected power from the probe detected jumps in the power spectra as the temperature varied from 265 to 282 K. For pure water, this jump occurred at 273 K, as seen in Figure 5. When the probe was in contact with a low-concentration salt solution (0.2% NaCl) however, the jump in absorbed power occurs at a lower temperature (272 K) . At all temperatures measured, the reflected power from the probe in the salt solution was around 0.175 dB lower than in pure water. Otherwise, the constant regions and 0.125 dB jump are consistent between the two samples.

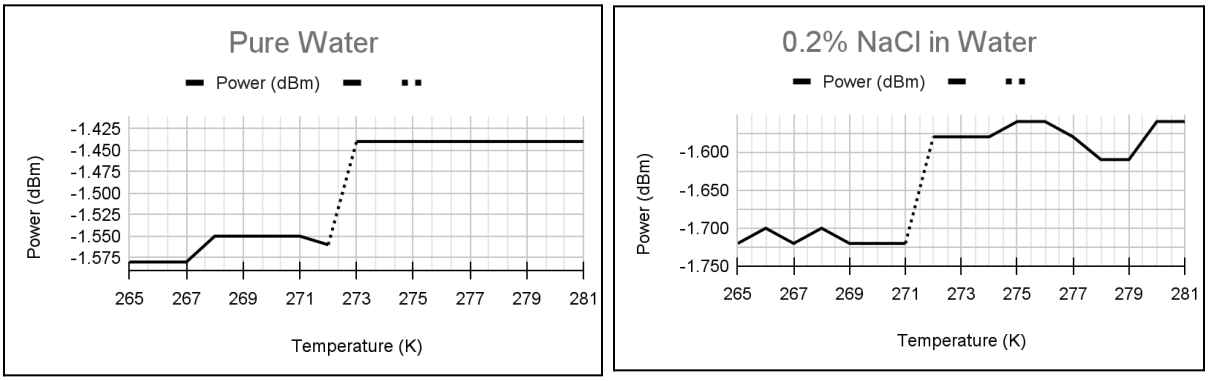

Figure 5. Temperature dependences on power absorption of pure water and 0.2% NaCl in water under 0 dBm, 1.0 GHz constant radiation. Temperature was controlled by using an ethylene glycol cooling bath and recorded with a thermocouple resting in bulk solution. Dashed lines show jumps in otherwise level spectra attributed to melting in the solution.

The semi-rigid probe also detected sensitive changes in sample properties of solutions of varying dimethylsulfoxide (DMSO; dielectric constant, 47, at 298 K) concentrations. At 260 K,

increases in the DMSO concentration were accompanied by more power absorption in the sample (Figure 6). The general trend of absorbed power versus DMSO concentration is consistent across the 1.0-1.6 GHz frequency range. The extent of increased power absorption varies depending on the frequency. At 1.0 GHz, the difference in reflected power is smaller than at 1.4 GHz.

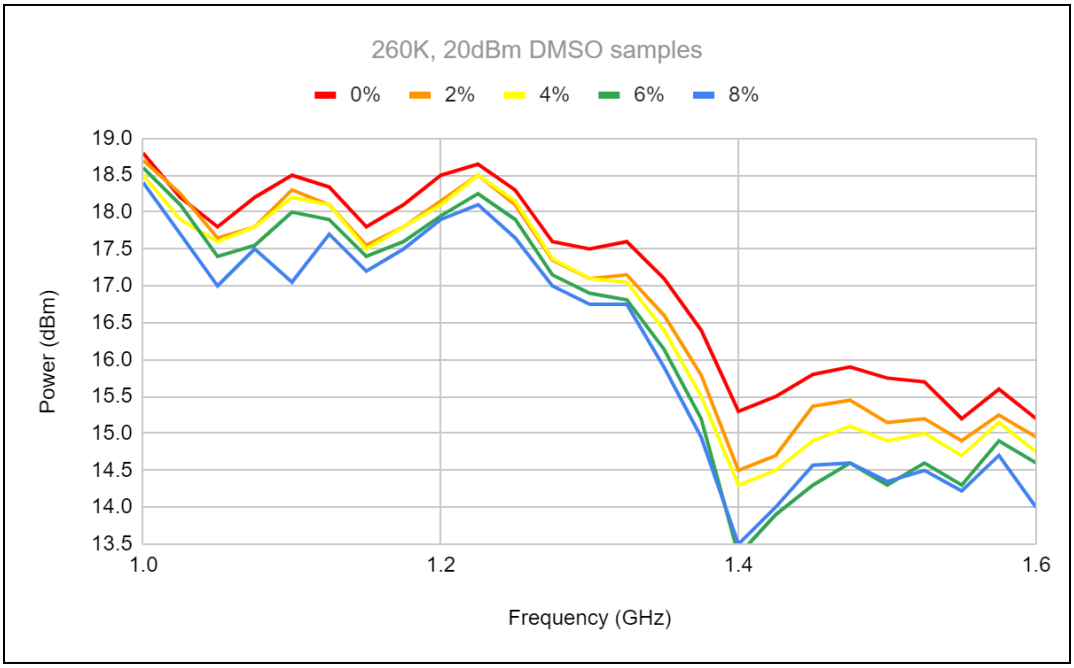

Figure 6. Power spectra for various DMSO concentrations (measured as v/v%) in water. For all samples, 20 dBm radiation was applied at 260 K. Measurements detected by semi-rigid coaxial cable with protruding center conductor embedded in 0.4 mL samples. Lines show a general trend of increased power absorption at higher concentrations, attributable to the increasing dielectric constant of the solution.

II. Actuation of solvent mobility in CW EPR experiment

At 120 K, acquisition of the EPR spectrum reveals the powder pattern lineshape. As the temperature increases, there is a characteristic narrowing in the lineshape. At temperatures above 200 K, application of 2 W (33 dBm) power results in noticeable changes to the line shape amplitude (Figure 7). At both 215 K and 235 K, the spectra collected from no probe power and 100 mW applied power (black and violet lines in Figure 7, respectively) are not visibly different. At 120 K and 200 K, all three power levels behave similarly.

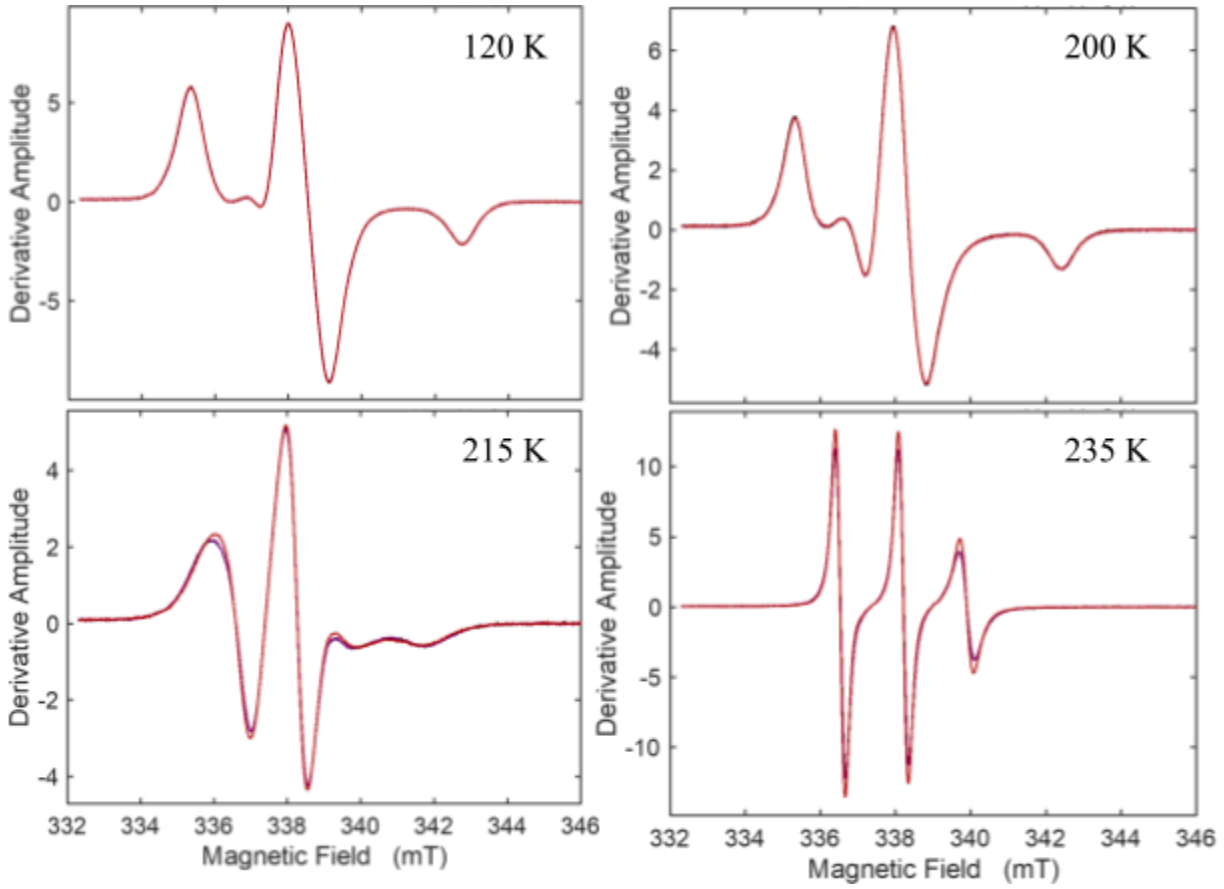

Figure 7. EPR spectra of TEMPOL with no probe power (black), 100 mW probe power (violet), and 2 W probe power (red) at 120 K, 200 K, 215 K, and 235 K. At each temperature, no significant difference between no power and 100 mW probe power is seen; however, at higher

temperatures, noticeable amplitude changes in the 2 W probe power line shapes are present, particularly at the low-field peak for the 215 K measurements. Relative derivative amplitudes for each temperature differ slightly.

III. Power dependence of solvent dynamical effect

The amplitude of EPR spectra increases as a function of the applied power. Figure 8 shows an overlay of the high-field resonance feature at 235K with 1.0 GHz frequency applied signal. Figure 9 shows the power dependence of the peak-to-trough amplitude differences in these spectra. There is a positive correlation between the applied probe power and the amplitude increase consistent across the entire spectrum at 235 K.

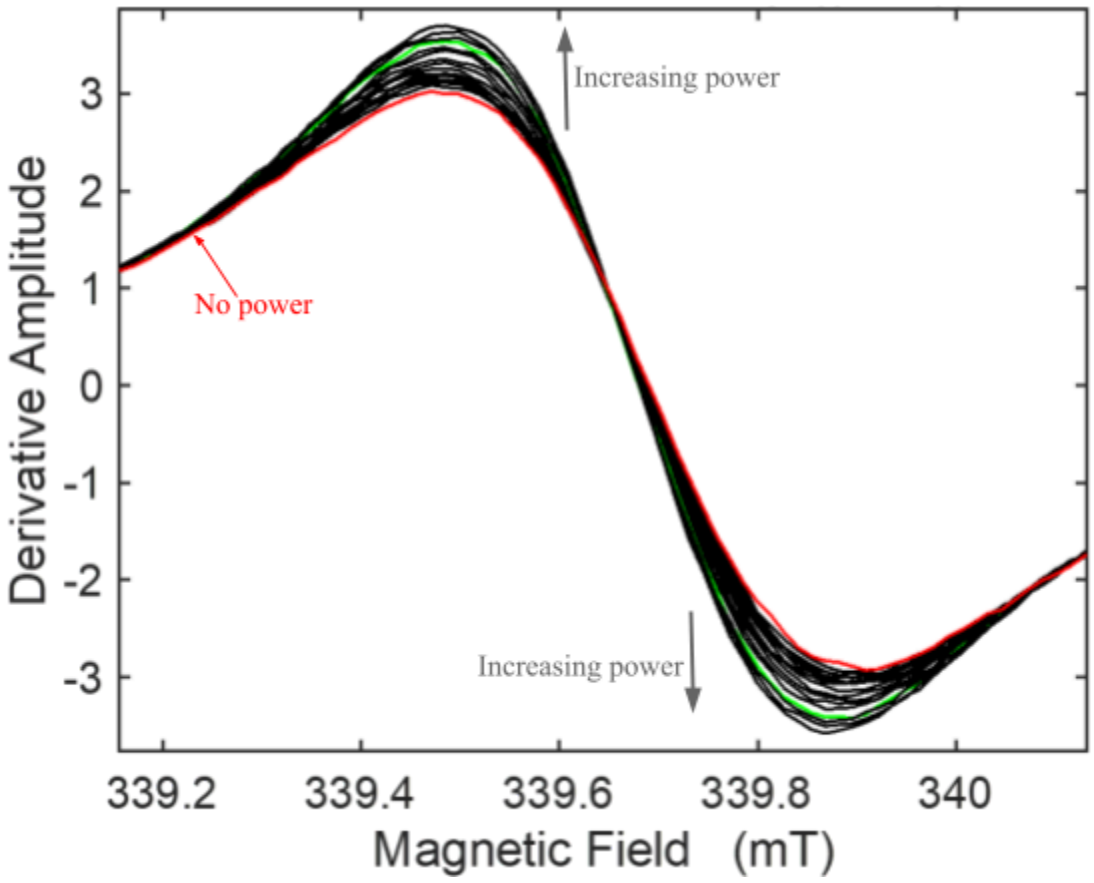

Figure 8. Power dependence of the high-field peak of EPR spectra of TEMPOL at 235 K. The red line is representative of no applied power. The green line corresponds to 2 W probe power, the maximum used in other tests. As the power increases, the peak-to-peak amplitude difference correspondingly increases. Each line is representative of a 1 dB increase in the applied power, going from 20 dBm to 35dBm.

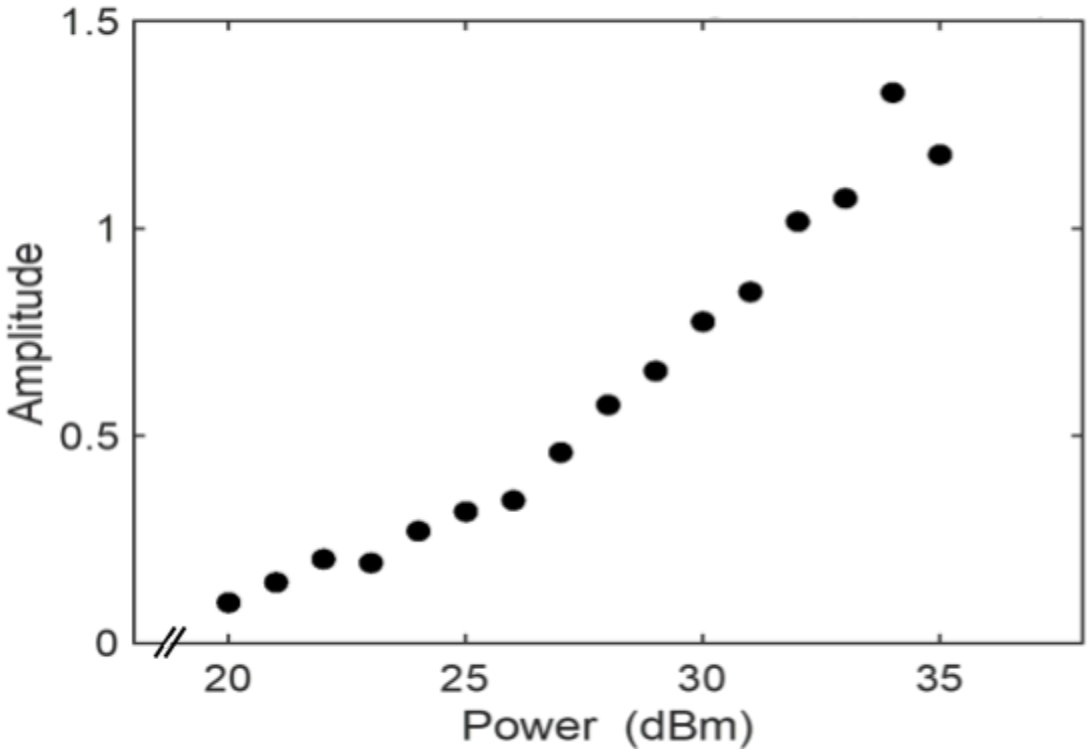

Figure 9. Peak-to-peak amplitude difference of the high-field first derivative spectrum as a function of the probe power. Higher power stretches the amplitude of both the peak and trough of the high-field feature.

IV. Frequency dependence of microwave dynamical effect

EPR spectra of TEMPOL at 235 K under 2 W incident probe power show an increase in amplitude at higher frequencies. Figure 10 shows the peak-to-trough amplitude difference increase as a function of the applied frequency for the high-field resonance peak. This trend is consistent across the entire EPR spectrum.

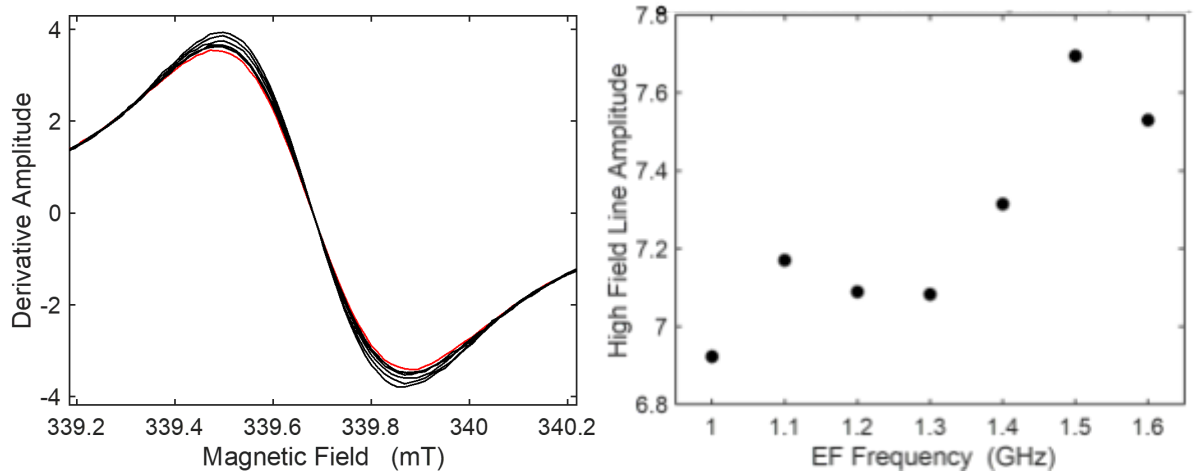

Figure 10. (left) Frequency dependence of the high-field peak of EPR spectra of TEMPOL at 235 K with a constant power level of 2 W. The red line corresponds to 1.0 GHz applied frequency. The frequency was increased to 1.6 GHz in increments of 0.1 GHz. (right) Peak-to-trough amplitude difference for high-field EPR spectra at different frequencies.

Discussion

I. Confirmation of appropriate microwave power absorption dependence on material dielectric properties

The measured power absorption difference between air and water in Figure 4, and between the different DMSO concentrations in Figure 6, are consistent the changes in associated

dielectric constants; materials with higher dielectric constants typically absorb more microwave power[18]. In Figure 4, water reflects a lower microwave power across the entire frequency range, attributable to its much higher dielectric constant. In Figure 6, this pattern repeats, owing to the dependence of the dielectric constant of DMSO water solutions on the concentration of DMSO[19]. At low temperature (<0 °C, <273 K), DMSO forms interstitial channels in the frozen water[16], allowing for pocket regions of material with higher microwave absorbance, and increasing DMSO concentrations lead to more microwave absorption. The detection of changes in dielectric properties is also verified by state change detections in Figure 5. Increasing the concentration of NaCl in water reduces the solution freezing point to <-1 °C, which is a more drastic change than anticipated from known effects of salt concentration on water's freezing point (expected shift <0.5 °C)[20]. The jump in absorbed power in the pure water curve associated with a detectable change in the solution properties occurs at 0 °C, the known freezing point of water. This jump happens at a lower temperature in the 0.2% NaCl solution, consistent with salt's effect on lowering freezing points in water. Additionally, while the two dependences on temperature share similarities, in that there are two flat regions with a similarly scaled jump, there is a 0.175 dB downward shift of the entire power spectrum in the salt concentration data, indicating more microwave absorption. Sodium chloride introduces more charges into the system, which are capable of interacting with the microwave *E*-field. This interaction could explain the small increase in power absorption.

II. Subtraction analysis of 235 K EPR spectra reveals effect of microwave irradiation on spin probe rotational motion

Acquisition of the EPR spectrum at 235 K under high-power microwave irradiation (2 W) at 1.0 GHz yields a small increase in spectrum amplitude for each resonance feature. In general, increased amplitude and narrowing of each of the three lines indicates an increase in spin probe rotational motion. Under the simple assumption that the rotational mobility of a small subset of the total spin probe population is increased, while the majority of the population maintains the mobility (and spectrum) established by the bulk solution temperature, subtraction of a scaled proportion of the zero power (P=0) spectrum will reveal the spectrum of the microwave-actuated population. Subtracting the spectrum acquired at P=0 yields non-physical EPR spectral features (Figure 11). This indicates an overcompensation in the subtraction, not accounting for the population of spin probe in the sample, whose mobility was not influenced by application of microwave power. To determine what fraction of the spin probe population in the sample "feels" the effects of the microwave irradiation, smaller fractions of the spectrum at P=0 were subtracted until deviations in the line shape baseline (example feature, red arrows in Figure 11) flattened-out into physically realistic features. This occurred when a proportion of 0.82 of the P=0 spectrum was subtracted from the high-power spectrum. This result implies that, at 235 K, 18% of the spin probe population in the sample is experiencing the effects of microwave irradiation. Similar analysis carried out on the collected spectra at 215 K (Figure 12) yielded activated population values of 8%. Carrying out the same procedure for 220 K and 240 K measurements show reactive percentages of the spin probe population of 14% and 20%. Overall, as the temperature increases, more of the corresponding P=0 spectrum is converted to the high-power spectrum, corresponding to an increase in the affected fraction of spin probe

population. Relatively small fractions of the population being affected are appropriate, considering the dimensions of the sample; the spin probe occupies a 1 cm length of the quartz tube, and studies using coaxial probes with similar geometrical and material properties have shown the strong, near-field region of the microwave signal has a penetration depth of ~1 mm[21]. As the temperature rises, the increased mobility in the solvent from thermal motion may allow TEMPOL molecules to be influenced by the weaker, far-field region of the probe.

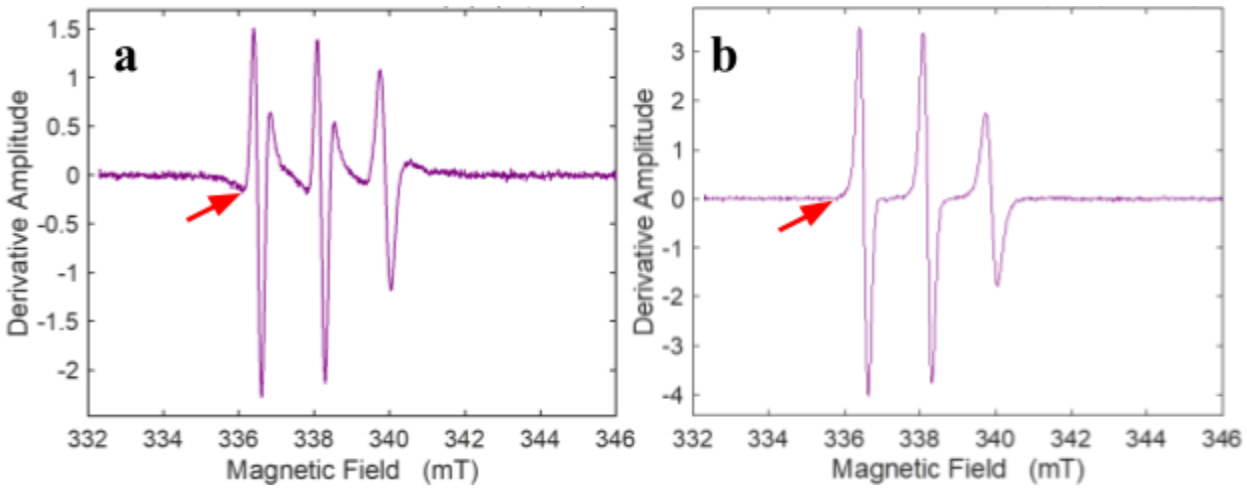

Figure 11. Resolution of the microwave radiation perturbed spectrum of the TEMPOL by using subtraction of scaled TEMPOL spectrum acquired in the absence of microwave radiation (P=0), at 235 K. (a) Result of subtracting EPR spectrum of TEMPOL at 235 K under no applied microwave power from EPR spectrum of TEMPOL at 235 K under 2 W, 1.0 GHz applied power. Red arrow points to one of several non-physical lineshape features resulting from subtraction of the unscaled P=0 spectrum. (b) Result of subtracting a scaled, 82% amplitude EPR spectrum of TEMPOL at 235 K under no applied microwave power from the EPR spectrum of TEMPOL at

235 K under 2 W, 1.0 GHz applied power. Red arrow points to the resolved lineshape feature resulting from subtraction.

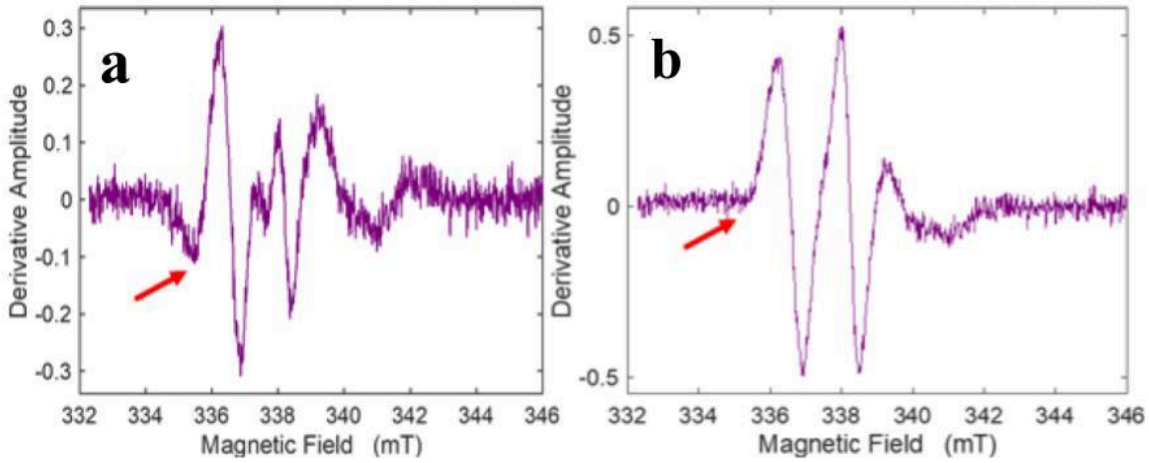

Figure 12. Resolution of the microwave radiation perturbed spectrum of the TEMPOL by using subtraction of scaled TEMPOL spectrum acquired in the above of microwave radiation, at 215 K. (a) Result of subtracting EPR spectrum of TEMPOL at 215 K under no applied microwave power from EPR spectrum of TEMPOL at 215 K under 2 W, 1.0 GHz applied perturbation. Red arrow points to one of several non-physical lineshape features resulting from subtraction of the unscaled P=0 spectrum. (b) Result of subtracting 92% amplitude of EPR spectrum of TEMPOL at 215 K under no applied microwave power from EPR spectrum of TEMPOL at 215 K under 2 W, 1.0 GHz applied radiation. Red arrow points to the example resolved lineshape feature resulting from subtraction.

III. Verification of line shape narrowing as an indicator of increased solvent mobility

Narrowing of EPR spectra generally accompanies the increase in amplitude, as a consequence of increased spin probe rotational motion. Therefore, to confirm that mobility is increased within

the solvent, the dependence of the peak-to-trough linewidth of the high-field hyperfine lineshape feature on microwave power was assessed. The peak and trough correspond to the inflection points in the microwave absorption lineshape. For the 235 K spectra, Figure 13 shows the general trend of the peak and trough of the high-field feature as a function of microwave power. As the incident power is increased, the maximum (peak) shifts slightly right while the minimum (trough) shifts slightly left. Thus, the two features move inward, and the collective trend is a narrowing of the high-field resonance feature, which is consistent with the increased spin probe and surrounding solvent mobility indicated by the increase in amplitude.

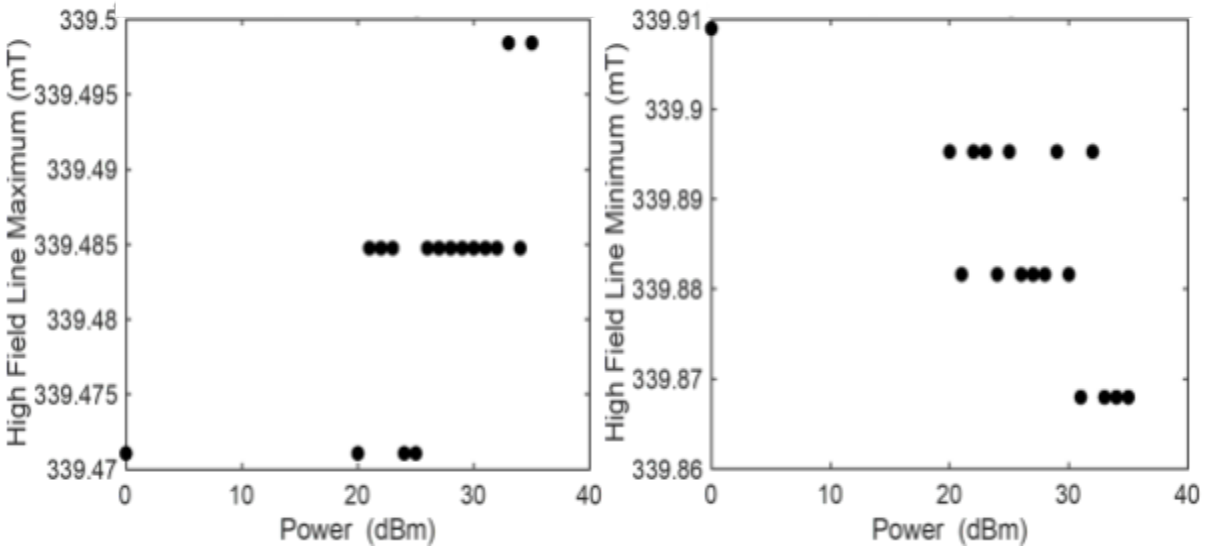

Figure 13. Figure 13. General trend of field-position shifts of the high-field resonance feature of TEMPOL spectra at 235 K. (Left) Dependence of the position of the maximum amplitude value of the peak feature on microwave power. (Right) Dependence of the position of the minimum amplitude value of the trough feature on microwave power. Microwave frequency: 1 GHz. The

data points occupy flat regions separated by a uniform increment, because of the limited point-to-point sampling resolution (aliasing) in the spectrum acquisition.

IV. Conclusions

Overall, we have shown an ability of the open-ended coaxial probe configuration to detect changes in the dielectric properties of the interstitial microstructure of frozen aqueous solutions of different composition, and to directly actuate solvent dynamics within the sample. The spin probe EPR spectra show a dependence of the extent of this effect on both the frequency (1.0 - 1.6 GHz) and power (0 - 2 W) of the microwave sample delivered. Increased microwave power increases the mobility of the EPR spin probe, as expected for an increase in the dynamics or motion in the surrounding aqueous solvent. The increased spin probe mobility with microwave frequency is also expected, based on the increase in microwave power absorption of water with increased frequency in the L- band (1.0 - 2.0 GHz) range[22]. At higher temperatures (235 K, relative to 215 K), increased freedom of the spin probe in its environment allows for a wider local range of effects of the microwave probe. From the current results, the origin of these effects, from either non-local thermal heating or localized charge motion, cannot be determined. Our demonstrated capability to directly actuate frequency-specific mobility changes in the solvent provides a promising forward direction for distinguishing this mechanism. The experimental system is also promising for application to examine the influence of microwave radiation, and actuation of "select" configurational fluctuations[11, 12], in the EAL system. Monitoring effects of our applied temperature-, power- and frequency-varied microwave

perturbation on reaction rate could lead to the resolution of different select fluctuations to enzyme catalysis, and an ability to drive enzyme turnover at faster rates in native and engineered non-native environments.

References

1. Microwave Heating - Mechanism and Theory. *CEM Corporation* (2024).
2. Gedye, R., Smith, F., Westaway, K., Ali, H., Baldisera, L., Laberge, L., & Rousell, J. The use of microwave ovens for rapid organic synthesis. *Tetrahedron Letters* **27**, 279–282 (1986).
3. Lin, S., Wu, C., Sun, M., Sun, C., & Ho, Y. Microwave-assisted enzyme-catalyzed reactions in various solvent systems. *Journal of the American Society for Mass Spectrometry* **16**, 581–588 (2005).
4. Young, D. D., Nichols, J., Kelly, R. M., & Deiters, A. Microwave activation of enzymatic catalysis. *Journal of the American Chemical Society* **130**, 10048–10049 (2008).
5. Copty, A. B., Neve-Oz, Y., Barak, I., Golosovsky, M., & Davidov, D. Evidence for a specific microwave radiation effect on the green fluorescent protein. *Biophysical Journal* **91**, 1413–1423 (2006).
6. Bren, U., Kržan, A., & Mavri, J. Microwave Catalysis through Rotationally Hot Reactive Species. *Journal of Physical Chemistry* **112**, 166–171 (2007).
7. Dudley, G. B., Richert, R., & Stiegman, A. E. On the existence of and mechanism for microwave-specific reaction rate enhancement. *Chemical Science* **6**, 2144–2152 (2015).
8. Broz, M., Oostenbrink, C., & Bren, U. The Effect of microwaves on protein Structure: Molecular Dynamics Approach. *Journal of Chemical Information and Modeling* **64**, 2077–2083 (2024).

9. Fenimore, P. W., Frauenfelder, H., McMahon, B.H., & Parak, F.G. Slaving: Solvent fluctuations dominate protein dynamics and functions. *Proceedings of the National Academy of Sciences* **99**, 16047-16051 (2002).
10. Frauenfelder, H., Chen, G., Berendzen, J., Fenimore, P. W., Jansson, H., McMahon, B. H. A unified model of protein dynamics. *Proceedings of the National Academy of Sciences* **106**, 5129 –5134 (2009).
11. Kohne, M., Li, W., Ionescu, A., Zhu, C., Warncke, K. Chapter Ten - Resolution and characterization of contributions of select protein and coupled solvent configurational fluctuations to radical rearrangement catalysis in coenzyme B12-dependent ethanolamine ammonia-lyase. *Methods in Enzymology* **669** 229-259 (2022).
12. Wei, L., Warncke, K. Native and nonnative reactions in ethanolamine ammonia-lyase are actuated by different dynamics. *Biophysics Journal* **122** 3976-3985 (2023).
13. Meaney, P. M., Gregory, A. P., Seppälä, J., Lahtinen, T. Open-Ended Coaxial Dielectric Probe Effective Penetration Depth Determination. *IEEE Transactions on Microwave Theory and Techniques* **64**, 915-923 (2016).
14. Li, Z., Zhou, L., Lei, H., Pei, Y. Microwave near-field and far-field imaging of composite plate with hat stiffeners. *Composites Part B: Engineering* **161**, 87-95 (2019).
15. Nforneh, B. & Warncke, K. Mesodomain and Protein-Associated Solvent Phases with Temperature-Tunable (200–265 K) Dynamics Surround Ethanolamine Ammonia-Lyase in Globally Polycrystalline Aqueous Solution Containing Dimethyl Sulfoxide. *Journal of Physical Chemistry* **121**, 11109–11118 (2017).
16. Nforneh, B. & Warncke, K. Control of Solvent Dynamics around the B12-Dependent Ethanolamine Ammonia-Lyase Enzyme in Frozen Aqueous Solution by Using Dimethyl

Sulfoxide Modulation of Mesodomain Volume. *Journal of Physical Chemistry* **123**, 5395–5404 (2019).

17. Ionescu, A., Li, W., Nforneh, B. & Warncke, K. Coupling of ethanolamine ammonia 54 lyase protein and solvent dynamics characterized by the temperature-dependence of EPR spin probe mobility and dielectric permittivity. *Journal of Physical Chemistry*. **154**, 175101 (2021).
18. Elmahaishi, M. F., Azis, R. S., Ismail, I., Muhammad, F. D. A review on electromagnetic microwave absorption properties: their materials and performance. *Journal of Materials Research and Technology* **20**, 2188-2220 (2022).
19. Yang, L., Yang, X., Huang, K., Jia, G., & Shang, H. Dielectric Properties of Binary Solvent Mixtures of Dimethyl Sulfoxide with Water. *International Journal of Molecular Science* **10**, 1261-1270 (2009).
20. Lamas, C. P., Vega, C., Noya, E. G. Freezing point depression of salt aqueous solutions using the Madrid-2019 model. *The Journal of Chemical Physics* **156**, 134503 (2022).
21. Sievert, B., Bott, J., Svejda, J. T., Pohl, N. Coaxial Cable Based Magnetic and Electric Near-Field Probes to Measure On-Chip Components up to 330 GHz. *IEEE Antennas and Wireless Propagation Letters* **99** 1-5 (2023).
22. Lyashchenko, A. K., Novskova, T. A. Structural dynamics of water and its dielectric and absorption spectra in the range 0–800 cm−1 *Journal of Molecular Liquids* **125**, 130-138 (2006).